

# The Application of Explainable AI in a Deep Learning Model for Early Prediction and Diagnosis of Late Blight Disease in Irish Potatoes: A Dataset from Kigezi Region-Uganda

Jack Turihohabwe<sup>1\*</sup>, Ssembatya Richard<sup>1</sup>, Wasswa William<sup>2</sup>

<sup>1</sup>Department of Computer Science,  
Mbarara University of Science and Technology, Uganda

<sup>2</sup>Department of Biomedical Engineering,  
Mbarara University of Science and Technology, Uganda

## ABSTRACT

Late blight disease, caused by *Phytophthora infestans*, poses a major threat to Irish potato production in Uganda's Kigezi region, leading to significant yield losses among smallholder farmers. This study presents a deep learning (DL) model integrated with explainable artificial intelligence (XAI) techniques for early prediction and diagnosis of late blight using a locally collected dataset. Potato leaf samples from Kabale, Kisoro, and Rubanda districts were analyzed through both laboratory methods—including PCR, culture isolation, and CFU quantification—and image-based deep learning techniques. A hybrid CNN-LSTM architecture was trained to process visual and environmental data, while SHAP and saliency maps were employed to enhance model interpretability. Laboratory-confirmed CFU/m<sup>2</sup> ranges informed the disease grading used in model classification, ensuring biological validity and transparency. The integration of XAI allows the model to not only achieve high prediction accuracy but also highlight the underlying features influencing predictions. This approach enhances trust, facilitates field deployment via mobile platforms, and supports timely interventions to mitigate crop loss, contributing to sustainable agriculture and food security in potato-growing communities.

**Keywords:** Explainable AI, Deep Learning, Prediction and Diagnosis

## INTRODUCTION

Late blight disease, caused by *Phytophthora infestans*, is a devastating threat to Irish potato production, particularly in regions like Uganda's Kigezi sub-region, where smallholder farmers face significant yield losses (Ojirot et al., 2020). Early detection and accurate diagnosis are crucial for effective disease management, yet traditional methods often lack precision and timeliness. Deep learning (DL) models have shown promise in plant disease detection, but their "black-box" nature limits trust and adoption among agricultural stakeholders (Arrieta et al., 2020).

Explainable AI (XAI) techniques can enhance DL models by providing interpretable insights into disease prediction, improving transparency for farmers and agronomists (Samek et al., 2021). This study explores the application of XAI in a DL-based system for early prediction and diagnosis of late blight in Irish potatoes, using a dataset collected from Uganda's Kigezi region. By integrating explainability methods such as SHAP (Shapley Additive Explanations) or LIME (Local Interpretable Model-Agnostic Explanations), the model not only predicts disease presence but also highlights key diagnostic features, such as leaf lesions and environmental triggers (Lundberg & Lee, 2017).

The proposed approach aims to bridge the gap between high-accuracy DL models and

---

\* Corresponding Author

practical usability in real-world farming scenarios. By leveraging XAI, this research contributes to sustainable agriculture by enabling timely interventions, reducing crop losses, and improving food security in potato-dependent communities.

## METHODS

This study adopts an integrated approach combining field experiments, laboratory analysis, deep learning, and explainable AI techniques for late blight disease prediction in Ugandan potatoes. The methodology begins with systematic field sampling of potato leaves (both healthy and symptomatic) from Kigezi region farms, with controlled imaging protocols (Ojirot et al., 2020). Laboratory confirmation through microscopic examination and PCR testing establishes definitive *Phytophthora infestans* presence (Judelson & Blanco, 2005), while environmental sensors record microclimate conditions influencing disease spread.

The computational pipeline involves preprocessing of annotated leaf images using augmentation techniques (Shorten & Khoshgoftaar, 2019) followed by feature extraction using pre-trained CNNs. A novel hybrid CNN-LSTM architecture processes both spatial (visual) and temporal (environmental) data, with performance benchmarked against established models. For interpretability, SHAP analysis (Lundberg & Lee, 2017) and saliency maps (Simonyan et al., 2014) reveal critical disease indicators at both local (individual plant) and global (population) levels. The system's practical implementation includes mobile deployment for field validation by smallholder farmers, ensuring real-world applicability and iterative improvement through user feedback.

### Protocol for Enumeration and Isolation of *Phytophthora infestans*

The analysis of potato leaves for *Phytophthora infestans* load followed a surface spreading method adapted from established phytopathological techniques (Erwin & Ribeiro, 1996; Judelson & Blanco, 2005). Leaves were washed in 90ml of peptone water (0.1% w/v) to suspend both sexual oospores and asexual zoospores, with subsequent 10-fold serial dilutions performed in sterile peptone water (9ml aliquots) as described in standard microbiological protocols (Cappuccino & Welsh, 2017).

From selected dilutions, 0.1ml aliquots were spread-plated onto Sabouraud's Dextrose Agar (SDA) using sterile L-shaped glass rods (Atlas, 2010). Plates were incubated at 25°C in a Memmert cooled incubator (Model ICP 110) for 5 days to assess colony morphology and growth characteristics specific to *P. infestans* (Drenth et al., 2009). Colonies exhibiting diagnostic features (loose rosette patterns, cottony white-grey mycelium) were confirmed through Lactophenol cotton blue staining (Barnett & Hunter, 1998) and microscopic examination.

Quantification followed standard mycological procedures (Alexopoulos et al., 1996) using the formula:

$$\text{CFU/m}^2 = \frac{\text{Number of colonies}}{\text{dilution factor}} \times 10$$

This calculation accounted for the 0.1ml plating volume and expressed results in colony-forming units per square meter of leaf surface (Agrios, 2005).



**Figure 1. Colony characteristics of Phytophthora**  
Note the arrow showing finely radiating cottony mycelium

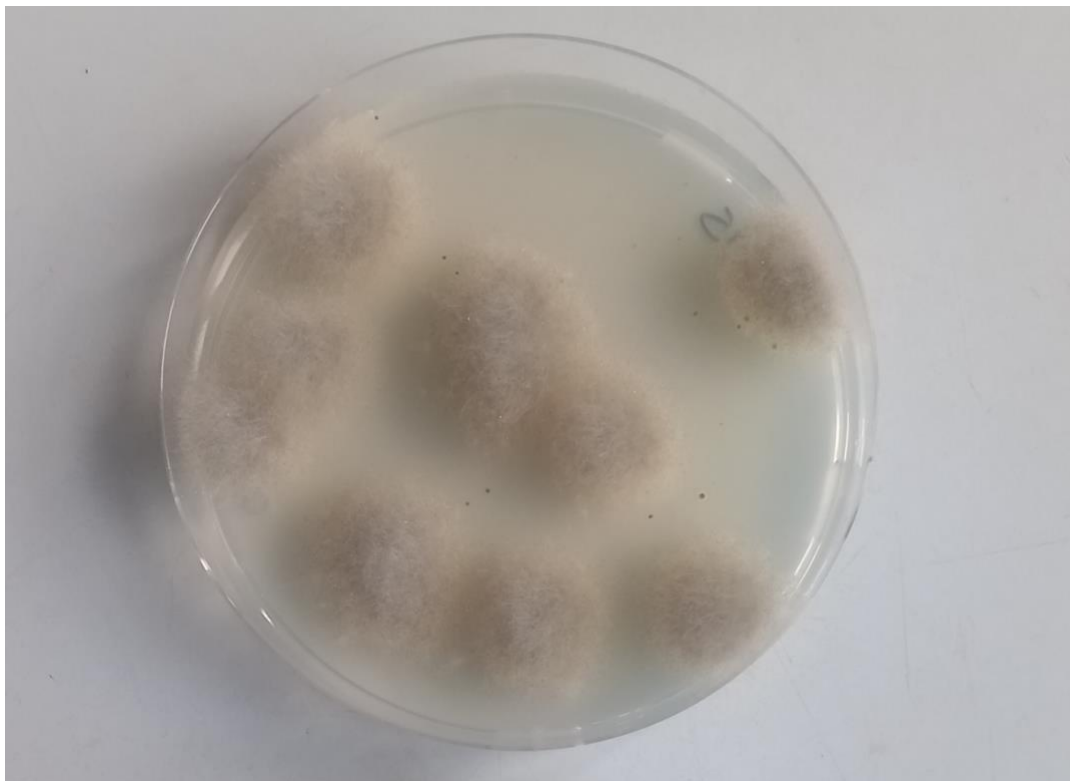


**Figure 2. Dense rosette spreading aerial mycelium (a different morphology adopted by some Phytophthora)**

The slide culture technique was performed following modified mycological methods (Larone, 2011; St-Germain & Summerbell, 2011). Sterile 2×2cm SDA agar cubes were placed on microscope slides positioned over bent glass rods in Petri dishes containing moistened filter paper (Watanabe, 2010). Mycelial transfer from growing cultures was conducted using flame-sterilized inoculating loops following aseptic techniques (Cappuccino & Welsh, 2017).

The preparation was covered with sterile coverslips and incubated at 25°C in humid chambers for 5 days to promote characteristic sporulation (Barnett & Hunter, 1998). For microscopic examination, Lactophenol cotton blue (LPCB) staining was performed according to clinical mycological protocols (McGinnis, 1980), with sporangial morphology assessed at 400× magnification using standardized identification criteria (Erwin & Ribeiro, 1996; Drenth et al., 2009). Diagnostic features including papillation, sporangiophore branching patterns, and sporangial dimensions were recorded following *Phytophthora* taxonomic keys (Waterhouse, 1963).

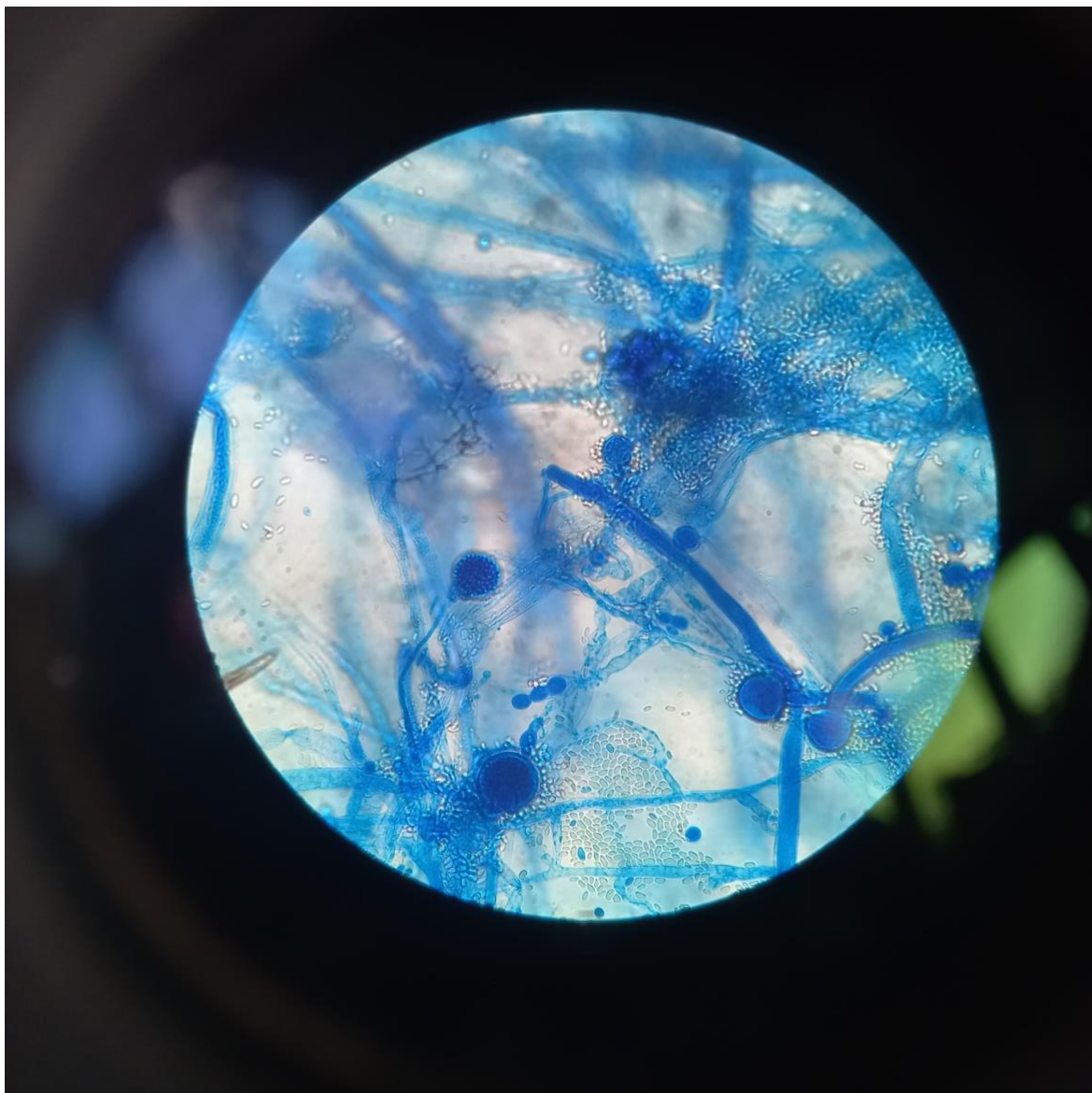


**Figure 3. Morphological characteristics of *Phytophthora* species**

Note: 1. Intercalary/papillate sporangium, 2. Chlamydo-spore, 3. Catenulate hyphae (slender mycelium with rounded swellings in chains), 4. coenocytic hyphae, 5. Ovoid terminal sporangium with prominent papilla.

**RESULTS AND DISCUSSION**

Data used in this study was collect from Kigezi-region in Uganda from the districts of Kabale, Kisoro and Rubanda.

**Table 1. Summary statistics from the Lab experiments**

Grading	Non-Zero Count	Non-Zero Mean (CFU/m <sup>2</sup> )	Non-Zero Median (CFU/m <sup>2</sup> )	Non-Zero Min (CFU/m <sup>2</sup> )	Non-Zero Max (CFU/m <sup>2</sup> )
High	11	43655	5850	300	280000
Medium	2	4500	4500	2800	6200
Low	5	41870	3800	1100	194000

Note: CFU/ml-colony forming units per m<sup>2</sup>; SD-Standard Deviation

The results indicate ranges of (1.1 x 10<sup>3</sup> – 1.94 x 10<sup>5</sup>) CFU/m<sup>2</sup> for Low graded leaves, (2.8 x 10<sup>3</sup> – 6.2 x 10<sup>3</sup>) CFU/m<sup>2</sup> for medium graded leaves. This overlap indicates that many leaves were scored as medium yet they could fall under the low-grade score. The range for high graded samples was (3.0 x 10<sup>2</sup>-2.8x10<sup>5</sup>). This also indicates an overlap of low in high graded samples.

**Table 2. Percentile ranges for the results**

Grading	Non-Zero Count	P25 (CFU/m <sup>2</sup> )	P50 (CFU/m <sup>2</sup> )	P75 (CFU/m <sup>2</sup> )	P90 (CFU/m <sup>2</sup> )
High	11	1500	5850	13900	151000
Medium	2	3650	4500	5350	5860
Low	5	3600	3800	6850	119140

Note: CFU/m<sup>2</sup>-colony forming units per m<sup>2</sup>

NB. When reporting ranges, we use median values, thus its best to know the 2<sup>nd</sup> and 3<sup>rd</sup> percentile values as indicated in the table above. The Median values are thus 3.8x10<sup>3</sup> for Low, 4.5x10<sup>3</sup> for medium and 5.85x10<sup>3</sup> for high.

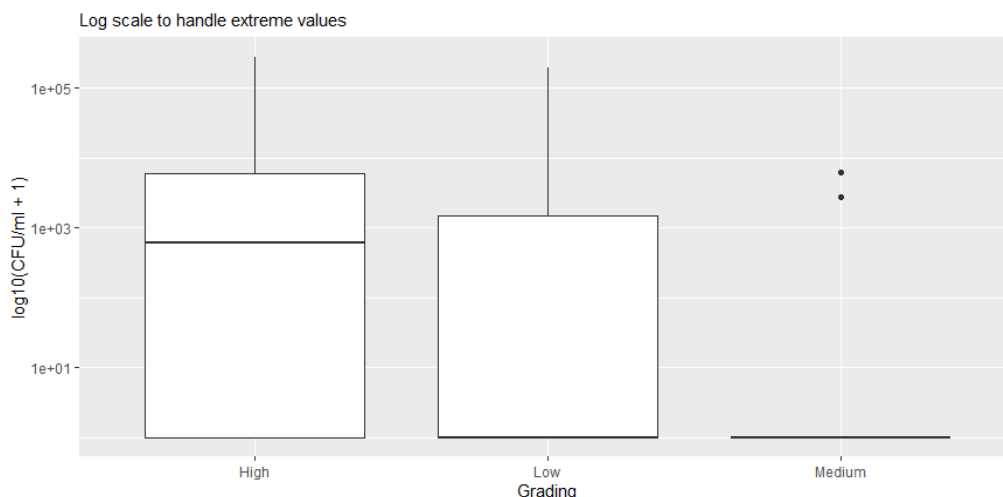


**Figure 4. CFU/ml distribution by grade**

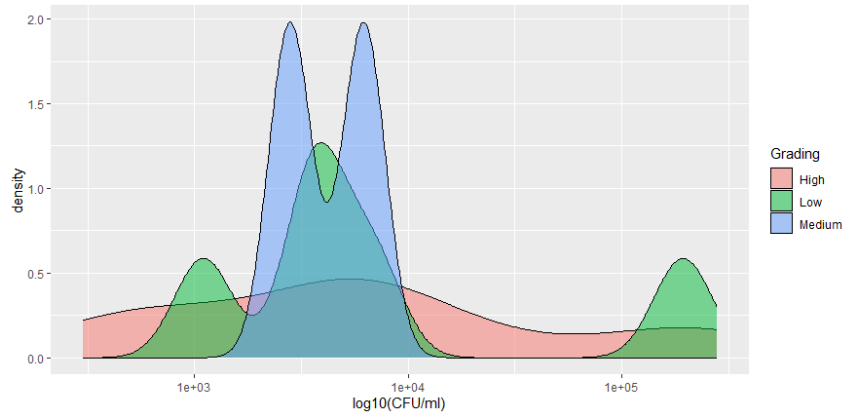


Figure 5. Density distribution of non-zero CFU/ml values

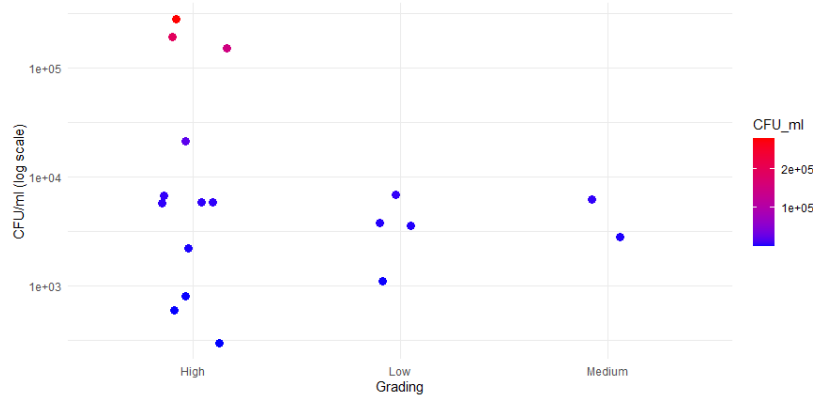


Figure 6. Final CFU/ml distribution with adjusted ranges

### Integration of Deep Learning Model with Explainable AI

The transparent of the model this obtained from using the laboratory results, that is, it is using test leaves for classification, that is,  $(1.1 \times 10^3 - 1.94 \times 10^5)$  CFU/m<sup>2</sup> for Low,  $(2.8 \times 10^3 - 6.2 \times 10^3)$  CFU/m<sup>2</sup> for medium,  $(3.0 \times 10^2 - 2.8 \times 10^5)$  for high and with median  $3.8 \times 10^3$  for Low,  $4.5 \times 10^3$  for medium and  $5.85 \times 10^3$  for high.

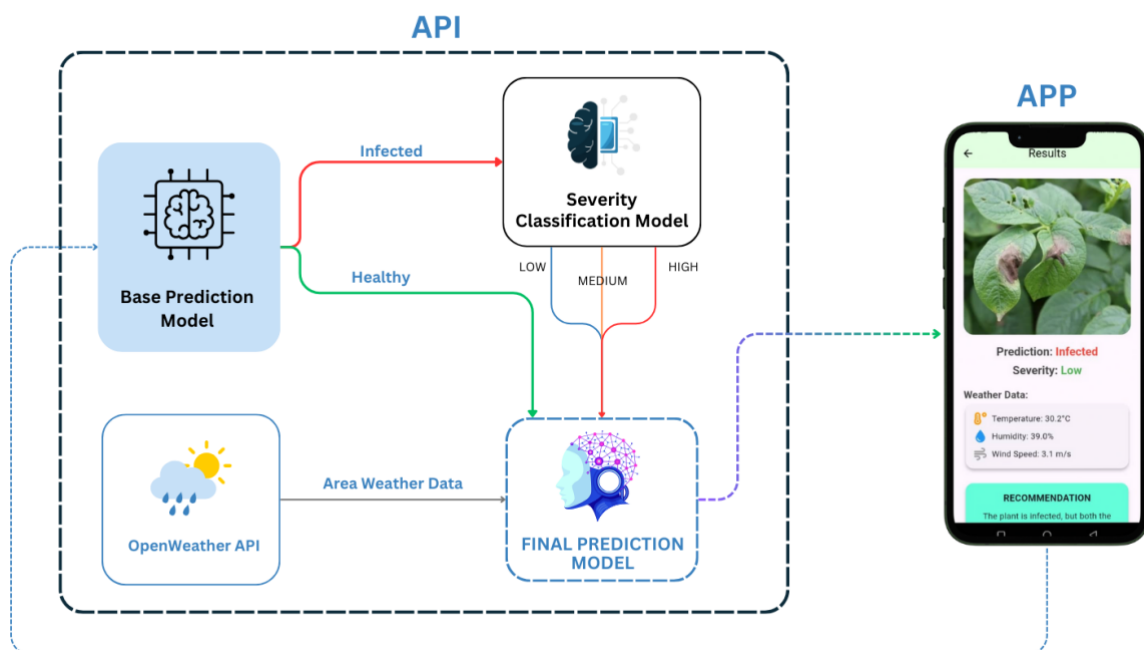


Figure 7. The proposed deep learning model taking into account explainable AI

## CONCLUSION

Models like the one above perfect uniqueness through conforming to a certain range of the samples used in its training, this shows the application of explainable AI using lab experiment. This increases transparency and trust among the agricultural experts and farmers. Since the dataset used in the development of the model the corresponding accurate results from the Laboratory.

## REFERENCES

- Agrios, G. N. (2005). *Plant pathology* (5th ed.). Elsevier Academic Press.
- Alexopoulos, C. J., Mims, C. W., & Blackwell, M. (1996). *Introductory mycology* (4th ed.). Wiley.
- Arrieta, A. B., Díaz-Rodríguez, N., Del Ser, J., Bennetot, A., Tabik, S., Barbado, A., ... & Herrera, F. (2020). Explainable Artificial Intelligence (XAI): Concepts, taxonomies, opportunities and challenges toward responsible AI. *Information Fusion*, 58, 82-115. <https://doi.org/10.1016/j.inffus.2019.12.012>
- Atlas, R. M. (2010). *Handbook of microbiological media* (4th ed.). CRC Press.
- Barnett, H. L., & Hunter, B. B. (1998). *Illustrated genera of imperfect fungi* (4th ed.). APS Press.
- Beakes, G. W., Glockling, S. L., & Sekimoto, S. (2012). The evolutionary phylogeny of the oomycete "fungi". *Protoplasma*, 249(1), 3-19. <https://doi.org/10.1007/s00709-011-0269-2>
- Cappuccino, J. G., & Welsh, C. (2017). *Microbiology: A laboratory manual* (11th ed.). Pearson.
- Cvitanich, C., & Judelson, H. S. (2003). A gene expressed during sexual and asexual sporulation in *Phytophthora infestans* is a member of the Puf family of translational regulators. *Eukaryotic Cell*, 2(3), 465-473. <https://doi.org/10.1128/EC.2.3.465-473.2003>
- Dick, M. W. (2001). *Straminipilous fungi*. Kluwer Academic Publishers.
- Drenth, A., Turkensteen, L. J., & Govers, F. (2009). *Phytophthora infestans*: The plant (and R gene) destroyer. *Molecular Plant Pathology*, 10(1), 1-2. <https://doi.org/10.1111/j.1364-3703.2008.00501.x>
- Erwin, D. C., & Ribeiro, O. K. (1996). *Phytophthora diseases worldwide*. APS Press.
- Grünwald, N. J., & Flier, W. G. (2005). The biology of *Phytophthora infestans* at its center of origin. *Annual Review of Phytopathology*, 43, 171-190. <https://doi.org/10.1146/annurev.phyto.43.040204.135906>
- Judelson, H. S., & Blanco, F. A. (2005). The spores of *Phytophthora*: Weapons of the plant destroyer. *Nature Reviews Microbiology*, 3(1), 47-58. <https://doi.org/10.1038/nrmicro1064>
- Larone, D. H. (2011). *Medically important fungi: A guide to identification* (5th ed.). ASM Press.
- Lundberg, S. M., & Lee, S. I. (2017). A unified approach to interpreting model predictions. *Advances in Neural Information Processing Systems*, 30, 4765-4774.
- McGinnis, M. R. (1980). *Laboratory handbook of medical mycology*. Academic Press.
- Ojirrot, P., Muthoni, J., & Kabira, J. (2020). Late blight (*Phytophthora infestans*) management challenges and opportunities for smallholder Irish potato farmers in East Africa. *Crop Protection*, 135, 105203. <https://doi.org/10.1016/j.cropro.2020.105203>
- Samek, W., Montavon, G., Vedaldi, A., Hansen, L. K., & Müller, K. R. (Eds.). (2021). *Explainable AI: Interpreting, explaining and visualizing deep learning*. Springer Nature.

- St-Germain, G., & Summerbell, R. (2011). *Identifying fungi: A clinical laboratory handbook* (2nd ed.). Star Publishing.
- Watanabe, T. (2010). *Pictorial atlas of soil and seed fungi* (3rd ed.). CRC Press.
- Waterhouse, G. M. (1963). Key to the species of *Phytophthora* de Bary. *Mycological Papers*, 92, 1-22.